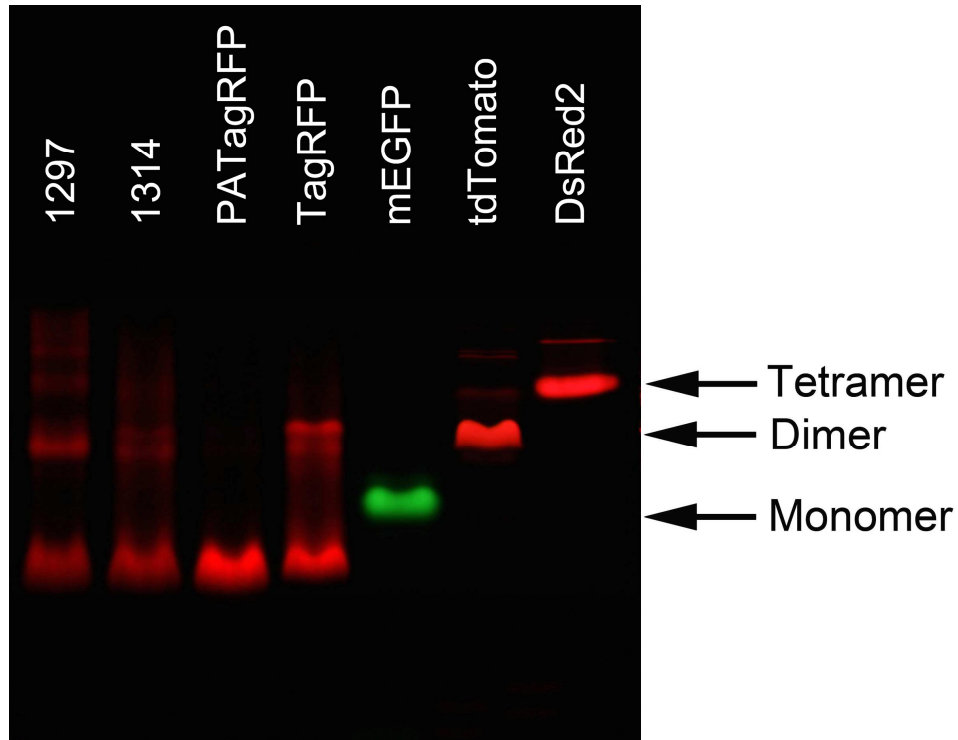


# Bright monomeric photoactivatable red fluorescent protein for two-color super-resolution sptPALM of live cells

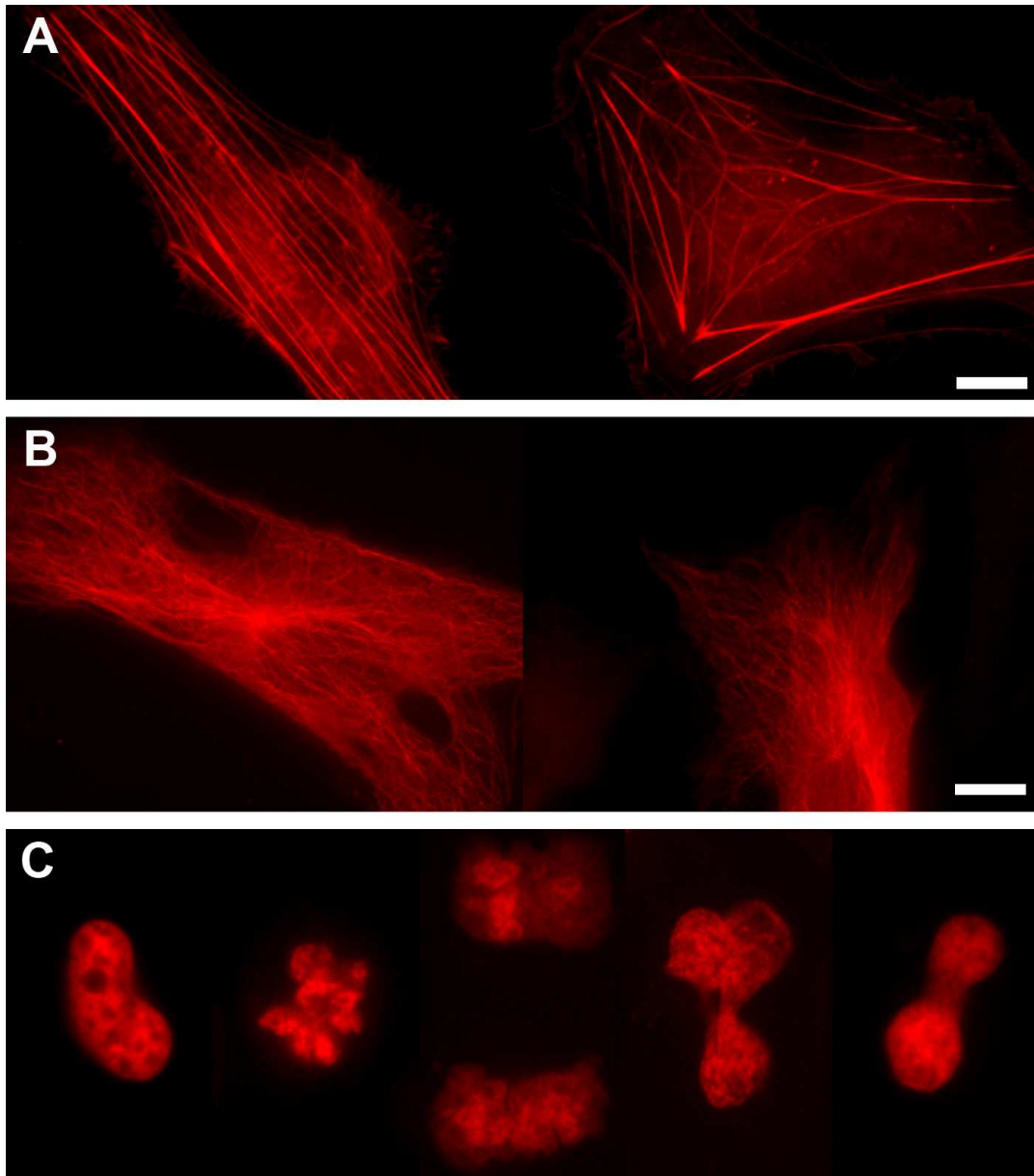
Fedor V. Subach, George H. Patterson, Malte Renz, Jennifer Lippincott-Schwartz and Vladislav V. Verkhusha

*Department of Anatomy and Structural Biology and Gruss-Lipper Biophotonics Center, Albert Einstein College of Medicine, 1300 Morris Park Avenue, Bronx, NY 10461, Biophotonics Section, National Institute of Biomedical Imaging and Bioengineering, National Institutes of Health, 9000 Rockville Pike, Bethesda, MD 20892, and Section on Organelle Biology, Cell Biology and Metabolism Program, National Institute of Child Health and Human Development, National Institutes of Health, 9000 Rockville Pike, Bethesda, MD 20892*

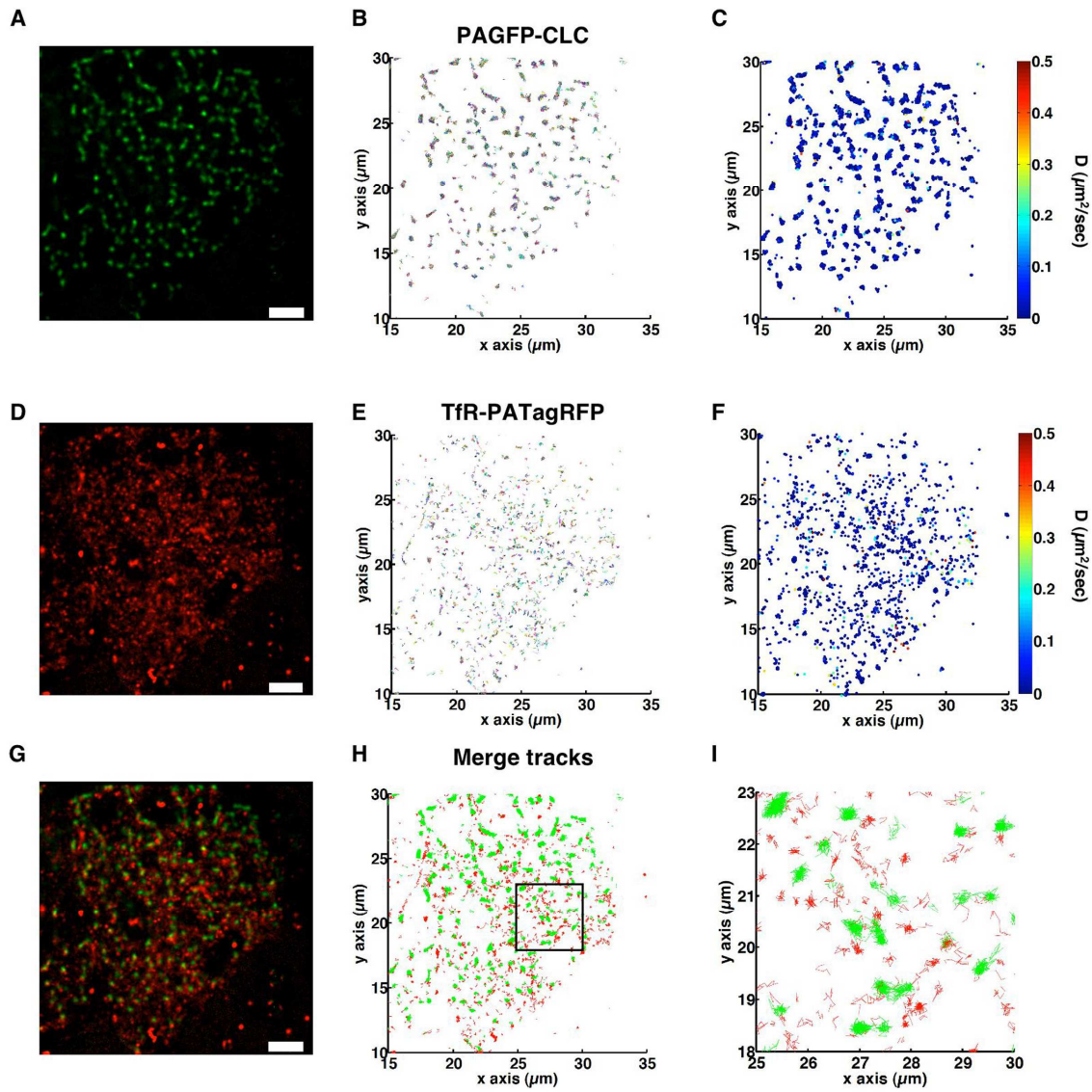
## **SUPPORTING INFORMATION**



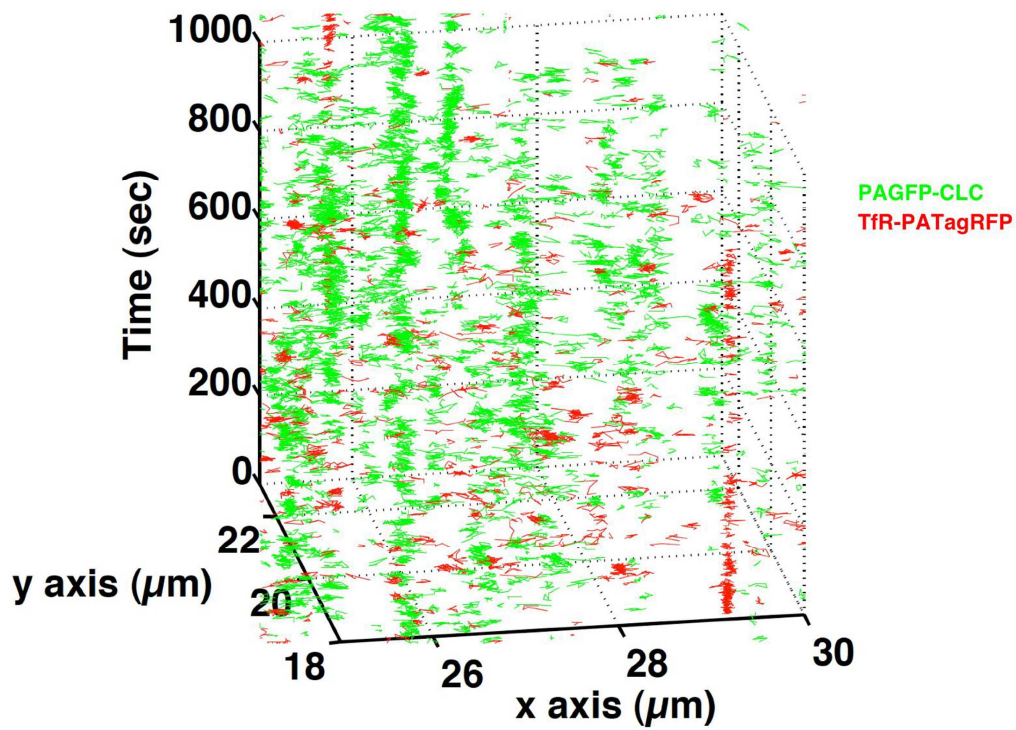
**Supporting Figure 1.** Semi-native polyacrylamide gel with PATagRFP variants. 10  $\mu\text{g}$  of the freshly purified fluorescent proteins were applied without heating in 10  $\mu\text{l}$  aliquots onto the 15% polyacrylamide gel containing 0.1% SDS. Before loading the PATagRFP variants were diluted till the equal concentrations of 1.9 mg/ml and photoactivated with the 405 nm LED array (50  $\text{mW}/\text{cm}^2$ ). The gel was run using a low voltage at  $+4^{\circ}\text{C}$ . mEGFP,<sup>1</sup> tdTomato<sup>2</sup> and DsRed2 (Ref.<sup>3</sup>) were applied as monomeric, dimeric and tetrameric native protein standards, respectively. The gel was photographed using a Leica MZ16FL fluorescence stereomicroscope.



*Supporting Figure 2.* Live HeLa cells expressing PATagRFP chimeras. Live HeLa cells expressing PATagRFP- $\beta$ -actin (A), PATagRFP- $\alpha$ -tubulin (B), and PATagRFP-histone-2B (C) were imaged after the photoactivation. Scale bars are 10  $\mu$ m.

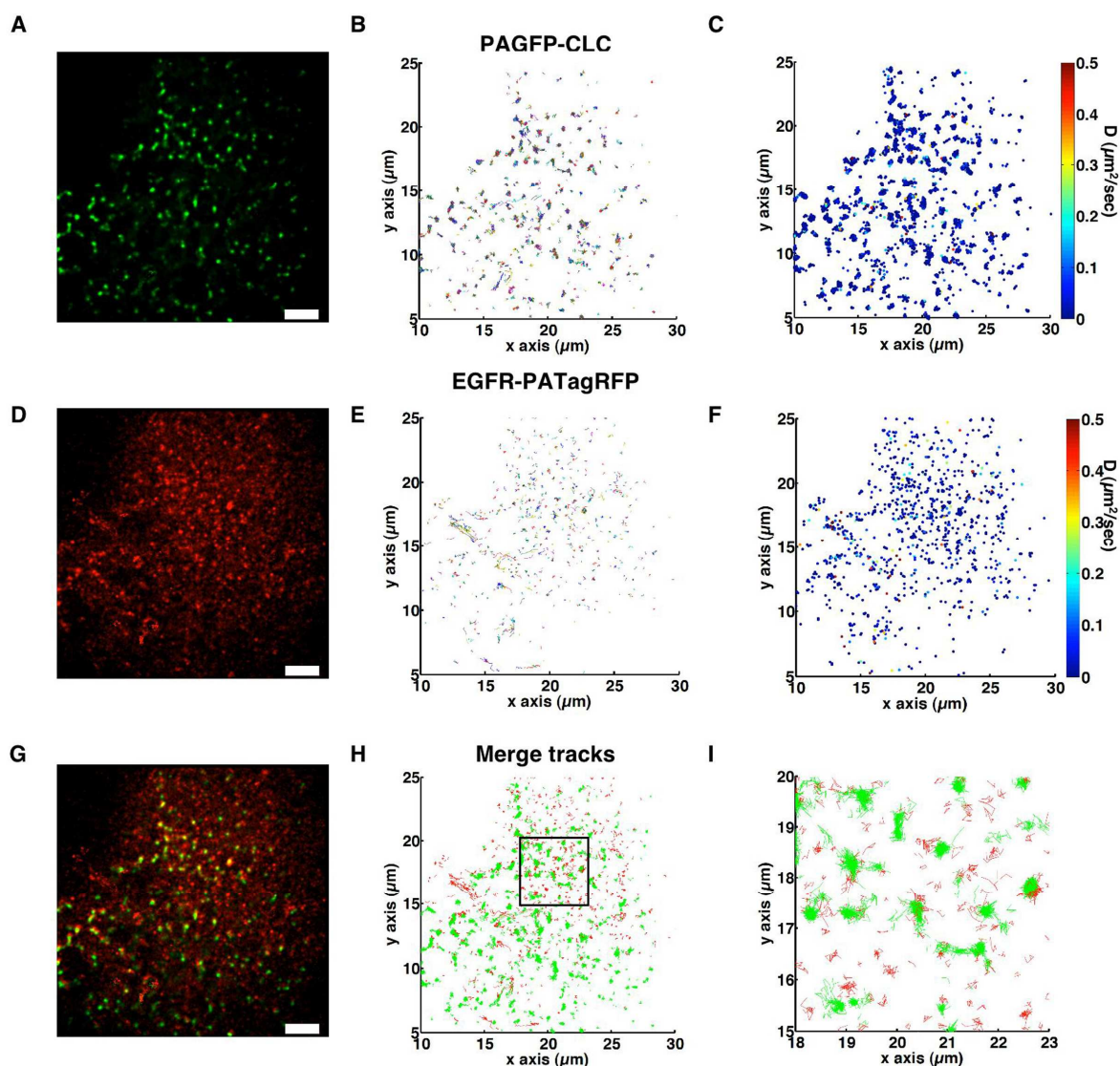


**Supporting Figure 3.** Two-color sptPALM: PAGFP-CLC and TfR-PATagRFP. (A-C) PAGFP-CLC and (D-F) TfR-PATagRFP were expressed in COS-7 cells and imaged by TIRF microscopy at 9.4 frames/sec under low levels of 561 nm excitation ( $<60 \text{ W/cm}^2$ ) and 405 nm photoactivation ( $<2.5 \text{ W/cm}^2$ ). PALM analysis was performed as previously published.<sup>4</sup> PALM images of (A) PAGFP-CLC (green) and (D) TfR-PATagRFP (red) are merged (G) to show the relative distributions of the molecules. Scale bars are  $2 \mu\text{m}$ . sptPALM analyses were performed as previously published.<sup>5</sup> Tracks of (B) PAGFP-CLC and (E) TfR-PATagRFP molecules lasting longer than 0.7 sec are plotted with each track represented by a different color. Mean squared displacements and diffusion coefficients were determined as previously published.<sup>5</sup> Diffusion coefficients are plotted for (C) PAGFP-CLC and (F) TfR-PATagRFP molecules at the start of the tracks and colored coded according to the color maps at the right. (H) PAGFP-CLC (green) and TfR-PATagRFP (red) tracks are merged. (I) A zoomed view of the region indicated by the square in (H). Approximately 2423 TfR-PATagRFP molecules were tracked along with  $\sim 7,222$  PAGFP-CLC molecules located in  $\sim 144$  pits.

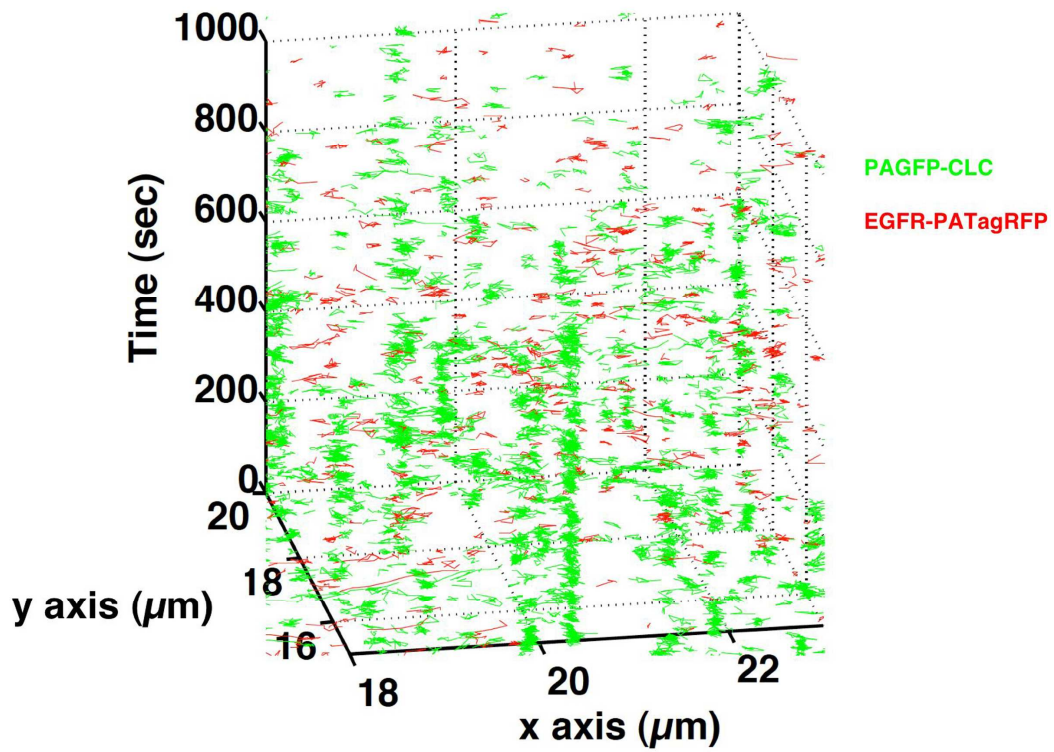


*Supporting Figure 4.* Three dimensional plot of PAGFP-CLC and TfR-PATagRFP two-color sptPALM. The x-y tracks of PAGFP-CLC and TfR-PATagRFP from Supporting Figure 3I are plotted as a function of time in the z-axis.

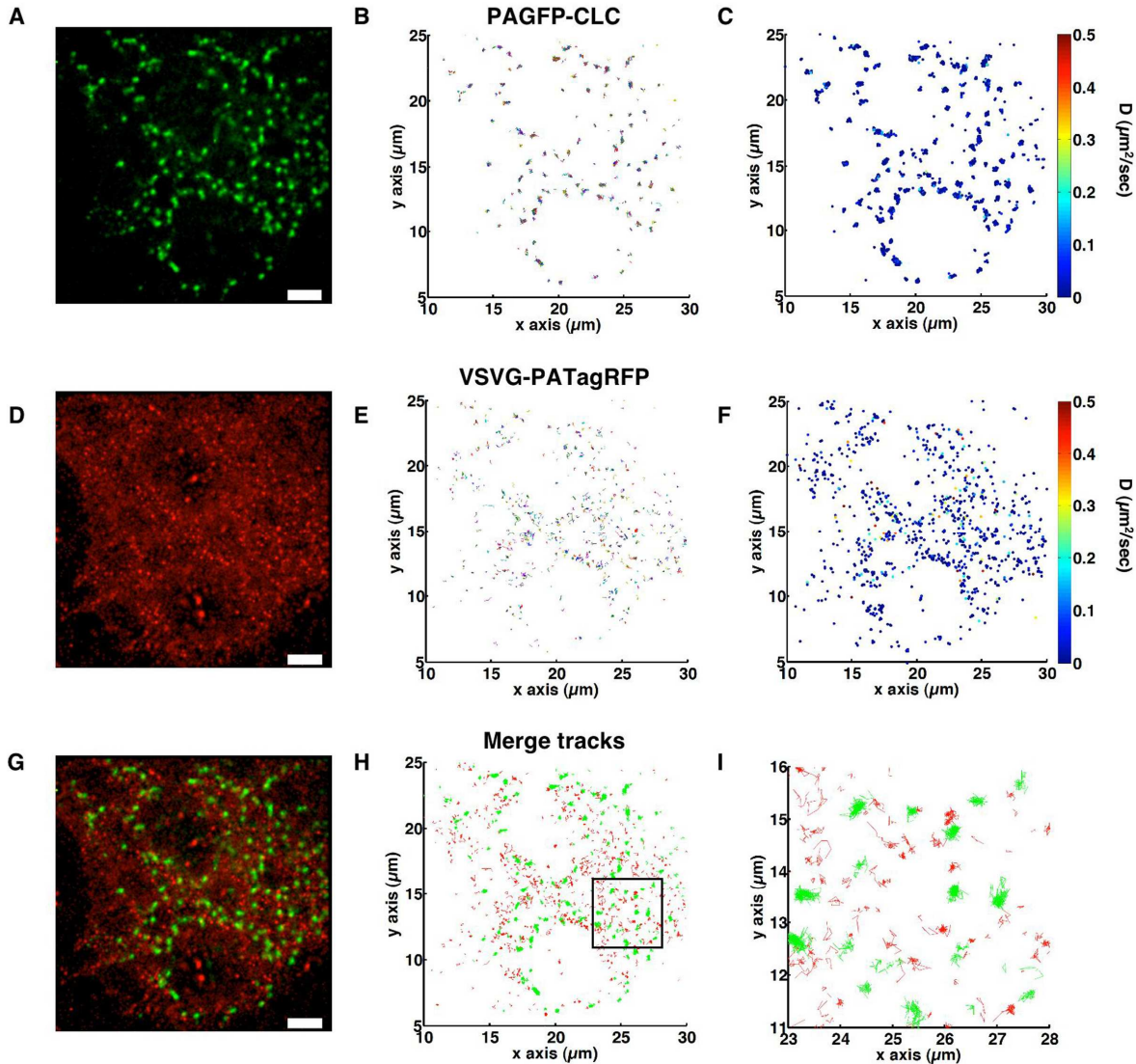




**Supporting Figure 5.** Two-color sptPALM: PAGFP-CLC and EGFR-PATagRFP. (A-C) PAGFP-CLC and (D-F) EGFR-PATagRFP were expressed and imaged as described for Supporting Figure 3. PALM analysis was performed as previously published.<sup>4</sup> PALM images of (A) PAGFP-CLC (green) and (D) EGFR-PATagRFP (red) are merged (G) to show the relative distributions of the molecules. Scale bars are 2  $\mu\text{m}$ . sptPALM analyses were performed as previously published.<sup>5</sup> Tracks of (B) PAGFP-CLC and (E) EGFR-PATagRFP molecules lasting longer than 0.7 sec are plotted with each track represented by a different color. Mean squared displacements and diffusion coefficients were determined as previously published.<sup>5</sup> Diffusion coefficients are plotted for (C) PAGFP-CLC and (F) EGFR-PATagRFP molecules at the start of the tracks and colored coded according to the color maps at the right. (H) PAGFP-CLC (green) and EGFR-PATagRFP (red) tracks are merged. (I) A zoomed view of the region indicated by the square in (H). Approximately 1034 EGFR-PATagRFP molecules were tracked along with  $\sim 5,181$  PAGFP-CLC molecules located in  $\sim 112$  pits.

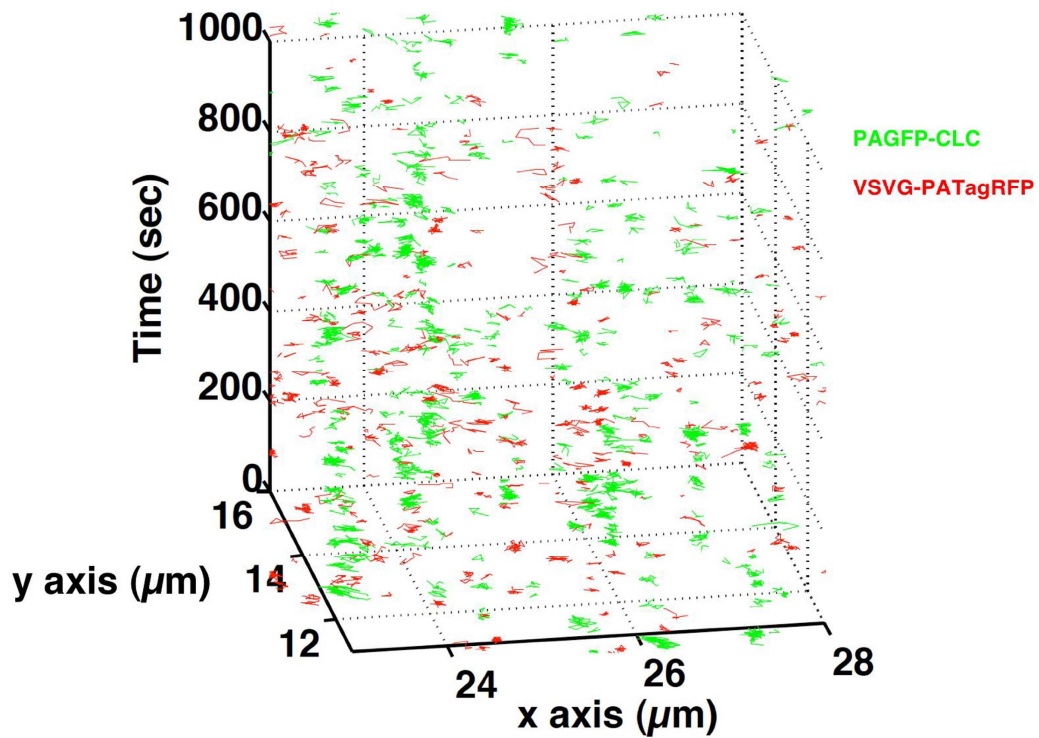


**Supporting Figure 6.** Three dimensional plot of PAGFP-CLC and EGFR-PATagRFP two-color sptPALM. The x-y tracks of PAGFP-CLC and EGFR-PATagRFP from Supporting Figure 5I are plotted as a function of time in the z-axis.



**Supporting Figure 7.** Two-color sptPALM: PAGFP-CLC and VSVG-PATagRFP. (A-C) PAGFP-CLC and (D-F) VSVG-PATagRFP were expressed and imaged as described for Supporting Figure 3. PALM analysis was performed as previously published.<sup>4</sup> PALM images of (A) PAGFP-CLC (green) and (D) VSVG-PATagRFP (red) are merged (G) to show the relative distributions of the molecules. Scale bars are 2  $\mu\text{m}$ . sptPALM analyses were performed as previously published.<sup>5</sup> Tracks of (B) PAGFP-CLC and (E) VSVG-PATagRFP molecules lasting longer than 0.7 sec are plotted with each track represented by a different color. Mean squared displacements and diffusion coefficients were determined as previously published.<sup>5</sup> Diffusion coefficients are plotted for (C) PAGFP-CLC and (F) VSVG-PATagRFP molecules at the start of the tracks and colored coded according to the color maps at the right. (H) PAGFP-CLC (green) and VSVG-PATagRFP (red) tracks are merged. (I) A zoomed view of the region indicated by the square in (H). Approximately 835 VSVG-PATagRFP molecules were tracked along with ~1292 PAGFP-CLC molecules located in ~86 pits.





**Supporting Figure 8.** Three dimensional plot of PAGFP-CLC and VSVG-PATagRFP two-color sptPALM. The x-y tracks of PAGFP-CLC and VSVG-PATagRFP from Supporting Figure 7I are plotted as a function of time in the z-axis.

## Supporting References

- (1) Zacharias, D. A.; Violin, J. D.; Newton, A. C.; Tsien, R. Y. *Science* **2002**, *296*, 913-916.
- (2) Shaner, N. C.; Campbell, R. E.; Steinbach, P. A.; Giepmans, B. N.; Palmer, A. E.; Tsien, R. Y. *Nat Biotechnol* **2004**, *22*, 1567-1572.
- (3) Terskikh, A. V.; Fradkov, A. F.; Zaraisky, A. G.; Kajava, A. V.; Angres, B. *J Biol Chem* **2002**, *277*, 7633-7636.
- (4) Betzig, E.; Patterson, G. H.; Sougrat, R.; Lindwasser, O. W.; Olenych, S.; Bonifacino, J. S.; Davidson, M. W.; Lippincott-Schwartz, J.; Hess, H. F. *Science* **2006**, *313*, 1642-1645.
- (5) Manley, S.; Gillette, J. M.; Patterson, G. H.; Shroff, H.; Hess, H. F.; Betzig, E.; Lippincott-Schwartz, J. *Nat Methods* **2008**, *5*, 155-157.